




 Cite this: *Chem. Commun.*, 2021, 57, 331

 Received 29th September 2020,  
 Accepted 23rd November 2020

DOI: 10.1039/d0cc06519f

rsc.li/chemcomm

# Organobase modulated synthesis of high-quality $\beta$ -ketoenamine-linked covalent organic frameworks†

 Rong Wang, Weifu Kong, Ting Zhou, Changchun Wang  and Jia Guo \*

**An organobase assisted approach is adopted to synthesize a series of  $\beta$ -ketoenamine-linked covalent organic frameworks (COFs), exhibiting superior crystallinity and porosity in comparison with those using an acidic catalyst. The quality promotion arises from the organobase-modulated transimination that favors the reaction kinetics for self-improvement of ordered structures.**

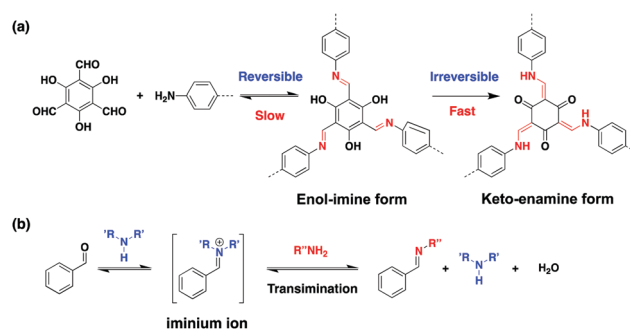
Covalent organic frameworks (COFs) are crystalline and porous frameworks that are emerging as a pre-designable platform to explore novel materials for advanced applications.<sup>1</sup> The kernel of COFs' synthesis is based on a reversible dynamic equilibrium to undergo an error-correcting route. However, the formed covalent linkages such as boronic esters and imine bonds suffer from instability in strong acid/base or protic solvents.<sup>2</sup> Thus, tremendous effort has been devoted to improving the chemical stability of linkages by a variety of strategies. Post-synthetic transformation of imine bonds towards amide, amine, oxazole, triazole, quinoline and so on is a flexible strategy to render the stability and multiple functionality.<sup>3–6</sup> However, the post-modification homogeneity has to be elaborately controlled for the 2D COFs with layered structures. In comparison, the bottom-up synthesis of chemically stable COFs based on  $sp^2$  C=C bonds,<sup>7,8</sup> phenazine rings<sup>9</sup> and  $\beta$ -ketoenamine linkers<sup>10,11</sup> can achieve more uniformity both in structure and composition. Furthermore, such 2D COFs could exhibit distinctive performances, especially for  $\beta$ -ketoenamine-linked COFs that possess electrochemical activity for energy storage applications.<sup>10,12,13</sup> Therefore, much attention has been paid to the exploration of  $\beta$ -ketoenamine-linked COFs.

Generally,  $\beta$ -ketoenamine units are formed by a reversible aldimine reaction of 1,3,5-triformylphloroglucinol (Tp) with aromatic amines, followed by a rapid enol-to-keto tautomerization

(Scheme 1a). The keto-enamine isomer is dominated in comparison with the enol-imine isomer. Hence the transformation process is almost irreversible.<sup>14</sup> This is unfavourable for structural rearrangement leading to a number of defective structures in the ordered domains of 2D COFs. Dichtel *et al.* proposed a monomer exchange approach to convert high-quality imine-linked COFs into  $\beta$ -ketoenamine-linked COFs with improved crystallinity and porosity.<sup>15</sup> Despite the pioneering study, a bottom-up strategy of improving the quality of such COFs has rarely been explored yet.

The typical catalyst for the synthesis of  $\beta$ -ketoenamine-linked COFs is acetic acid aqueous solution (6 M), which can activate carbonyl groups to undergo the nucleophilic reaction with amines. As an alternative, it has been reported that aminocatalytic methods are available for the direct preparation of aldimines by a transimination between iminium ions and amines (Scheme 1b).<sup>16</sup> This motivated us to study the structural evolution of  $\beta$ -ketoenamine-linked COFs in a pure organic system without addition of acidic aqueous solution.

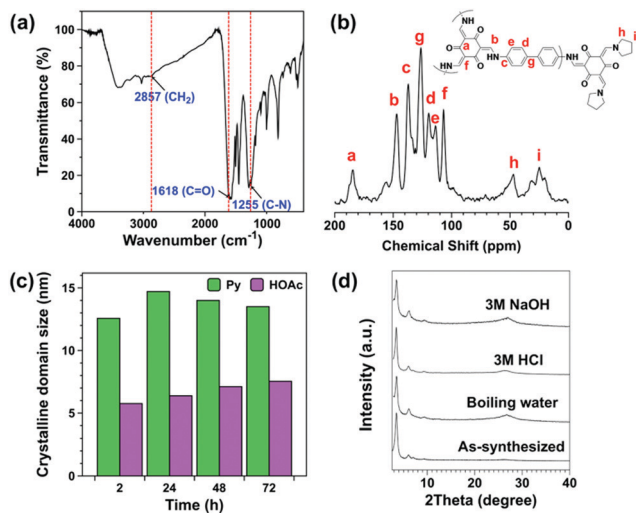
We adopted pyrrolidine (Py) as a representative to assist the synthesis of the typical  $\beta$ -ketoenamine-linked COF under solvothermal conditions. TpBD-COF consisting of Tp at the nodes and benzidine (BD) at the struts was prepared in a mixture of Py, *n*-BuOH and dichlorobenzene (1/1/9, v/v). The initial mixture quickly generated a precipitate at room temperature and



**Scheme 1** Illustration of (a) formation of  $\beta$ -ketoenamine linkage in COFs and (b) aldimine *via* an iminium ion intermediate.

State Key Laboratory of Molecular Engineering of Polymers,  
 Department of Macromolecular Science, Fudan University, Shanghai 200433,  
 P. R. China. E-mail: guojia@fudan.edu.cn

† Electronic supplementary information (ESI) available: Materials and methods, Fig. S1–S9, Scheme S1 and Tables S1 and S2. For ESI and crystallographic data in CIF or other electronic format see DOI: 10.1039/d0cc06519f



**Fig. 1** (a) FT-IR spectrum and (b) solid-state CP/MAS  $^{13}\text{C}$  NMR spectrum of TpBD-COF (Py). (c) The estimated average sizes of crystalline domains for TpBD-COF synthesized with HOAc aq. (6 M) and Py, respectively. (d) PXRD patterns of TpBD-COF (Py) treated with various media.

then the temperature was kept at 120 °C in a degassed Pyrex tube for a given time (see details in Table S1, ESI $^\dagger$ ). The resulting TpBD-COF was characterised by different techniques. FT IR spectra showed the characteristic vibrations of alkyl C–H, C=O and C–N bonds that appeared at 2857, 1618 and 1255  $\text{cm}^{-1}$ , respectively (Fig. 1a). Also, the solid-state CP/MAS  $^{13}\text{C}$  NMR spectrum displayed multiple peaks that could be assigned to the phenyl C (c, g, d and e) at 137.1, 126.5, 119.6 and 113.5 ppm, keto C (a) at 184.6 ppm, enamine C (b and f) at 146.9 and 106.8 ppm and alkyl C (h and i) at 46.9 and 24.9 ppm, respectively (Fig. 1b). The findings prove the formation of  $\beta$ -ketoenamine linkages. The presence of alkyl groups might be originated from the residual Py. We suppose that Py may react with the terminal aldehydes, leading to the end capping of the COF frameworks.

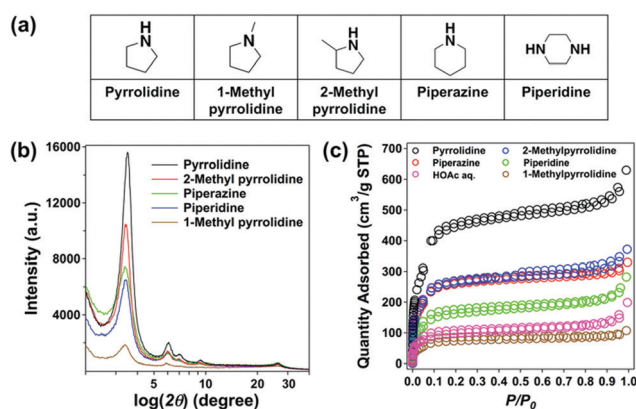
PXRD patterns demonstrated that the resulting COFs synthesized in the presence of Py had a typical hexagonal lattice as previously reported using an HOAc aq. catalyst (Fig. S1 in the ESI $^\dagger$ ).<sup>11</sup> All the diffraction peaks could be indexed to the (100) plane at 3.5°, (110) at 6.1°, (200) at 7.1°, (210) at 9.3° and (001) at 26.3°, respectively. Compared with the acidic system, the Py-assisted synthesis remarkably improves the crystallinity of the products (Fig. S2 in the ESI $^\dagger$ ). As shown in Fig. 1c, the average size of the (100) domain determined by Scherrer analysis<sup>17</sup> reaches 12.6 nm just at 2 h, which is almost double that of the COFs using an HOAc catalyst (5.8 nm). Furthermore, as the reaction was prolonged, the (100) crystalline domains were kept in the range of 13–15 nm. In contrast, the acid-catalytic crystallization gradually evolved in 72 h and eventually, the size of the crystalline domain was achieved to be as low as 7.5 nm. This implies that Py alters the reaction kinetics, which may facilitate the self-improvement of ordered structures. Then the chemical stability was testified by suspending the TpBD-COF powders in 3 M HCl, 3 M NaOH aq. and boiling water, respectively, for 7 days. It can be seen that all of the PXRD

patterns remained, indicative of the stability of  $\beta$ -ketoenamine linkages (Fig. 1d). Additionally, the treated solids could keep the original weights (>98%) and the remaining solutions were analysed by FT IR measurement, revealing that a trace amount of Py was present after the treatment of COFs with the given solutions (Fig. S3 in the ESI $^\dagger$ ). This may be attributed to the elimination of the terminal Py moiety on the frameworks.

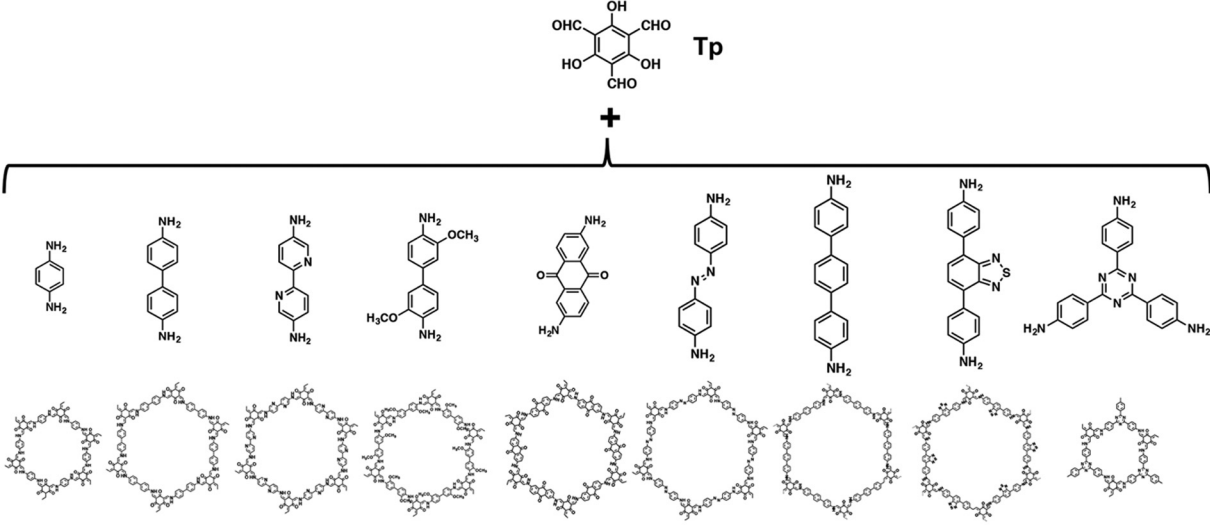
To further optimize the organobase assisted reaction, the effect of Py concentration on the crystallinity and porosity of COFs was studied. With an increase of Py from 0.50 to 9.09 vol% relative to a total of solution volume, the optimal PXRD pattern was achieved in the presence of 1.96 vol% Py (Fig. S4 in the ESI $^\dagger$ ) and accordingly, the Brunauer–Emmett–Teller (BET) surface area was as high as 2157  $\text{m}^2 \text{g}^{-1}$  (Fig. S5 in the ESI $^\dagger$ ). When the added Py was over 1.96 vol%, both the yields and quality of the COFs had been reduced to some extent. It is assumed that the high concentration of Py can increase the polarity of the reaction solutions (*n*-BuOH/dichlorobenzene, *v/v* = 1/9) and accordingly the solubility of the monomers and oligomers, thus causing an adverse effect on the crystallization of TpBD-COFs.

Next, we adopted a variety of organobases including piperidine, piperazine, 1-methylpyrrolidine and 2-methylpyrrolidine for the synthesis of TpBD-COF under otherwise identical conditions (Fig. 2a). All of them provided similar PXRD patterns, while the signal intensity at the main peak (3.5°) was considerably different (Fig. 2b). 1-Methyl Py, which is the tertiary amine, conferred the weakest X-ray diffraction intensity. Among the secondary cyclic amines, the five-membered Py was much more efficient than the six-membered piperazine and piperidine for the COF's crystallization. Additionally, 2-methyl Py led to a slightly weaker crystallinity than Py probably due to its steric hindrance effect.

The porosity of the COFs was studied by  $\text{N}_2$  sorption isotherms at 77 K. Fig. 2c displays the type IV-like adsorption for all of the COFs, indicative of the mesopore character. The use of Py led to a maximum in  $\text{N}_2$  adsorbed quantity, followed by 2-methyl Py, piperazine, piperidine, HOAc aq. and 1-methyl Py (Table S2 in the ESI $^\dagger$ ). The calculated BET surface areas of TpBD-COF reached as high as 2157  $\text{m}^2 \text{g}^{-1}$  in the presence of



**Fig. 2** (a) A series of organobases used for the synthesis of TpBD-COFs, and (b) PXRD patterns and (c)  $\text{N}_2$  sorption isotherms of those COFs.

Table 1 BET surface areas of a series of  $\beta$ -ketoenamine-linked COFs synthesized with Py and HOAc aq. (6 M), respectively


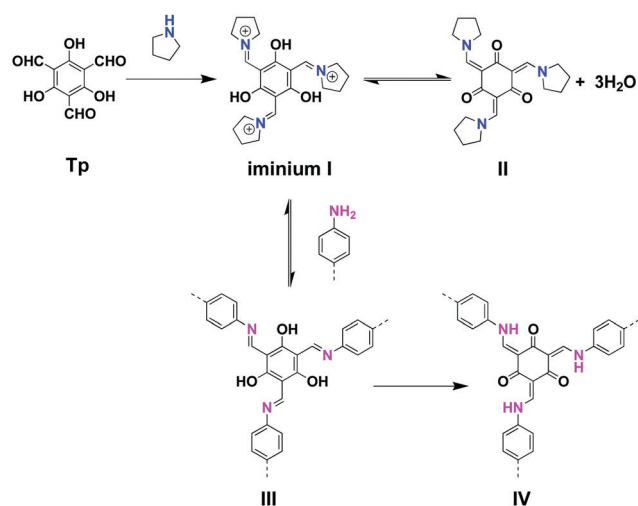
	$S_{\text{BET}}$ ( $\text{m}^2 \text{g}^{-1}$ )								
	TpPa	TpBD	TpBPy	TpBD(OMe) <sub>2</sub>	TpDAAQ	TpAzo	TpTP	TpBT	TpTAP
Pyrrolidine	684	2157	760	394	230	1520	1266	1022	867
HOAc aq. (6 M)	715	572	999	80	674	628	93	81	696

Py, which was roughly four times higher than that using HOAc as a catalyst ( $572 \text{ m}^2 \text{ g}^{-1}$ ). Also, 2-methyl Py and piperazine performed well in terms of apparent surface areas, which were around  $1000 \text{ m}^2 \text{ g}^{-1}$ . Among all the bases, 1-methyl Py gave the lowest surface area of  $298 \text{ m}^2 \text{ g}^{-1}$ . The pore-size distribution for the optimal PyBD-COFs was populated around 2.1 nm, which is in line with that earlier reported (Fig. S6 in the ESI†).

To corroborate the adaptability of organobases for the various  $\beta$ -ketoenamine-linked COFs, we expanded the amine monomers to react with Tp. Table 1 displays the nine kinds of COFs synthesized using Py and HOAc (6 M aq.), respectively, under otherwise identical conditions. It is evident that their crystallinity and porosity are significantly different (Fig. S7 and S8 in the ESI†). In many cases, Py is better than HOAc (6 M aq.) for crystallizing the COFs. The resulting COFs including TpBD, TpBD(OMe)<sub>2</sub>, TpAzo, TpTP, TpBT and TpTAP can give larger BET surface areas than the acid-catalysed counterparts. Furthermore, it is noted that Py appears to be more efficient for the synthesis of TpBT COF that is challenging when using HOAc.<sup>18</sup> Meanwhile, we are aware that the surface areas of TpPa COF are similar to those obtained in the acid or base system, whereas for TpBPy and TpDAAQ, the use of Py leads to relatively smaller surface areas. It was observed that the addition of Py largely improved the solubility of amine monomers in a mixed organic solution because of the H-bonding interaction between Py and the proton-accepting moieties, *i.e.* BPy and DAAQ. Thus, the reaction may be accelerated and unfavourable for crystallization based on a slow thermodynamic route.

To understand the role of organobases, a model reaction of Tp with Py proceeded in ethanol at room temperature. With the addition of Py, it was observed that Tp could completely

dissolve in ethanol. The solution was then treated to give a yellow solid. <sup>1</sup>H NMR demonstrated that it was compound **II** obtained with 92% yield (Fig. S9 in the ESI†), as shown in Scheme 2. It has been reported that aniline and its derivatives are used as a modulator to induce competition and enhance reversibility for the synthesis of challenging systems.<sup>19</sup> Hence, we propose a possible mechanism to understand the organobase-assisted synthesis of  $\beta$ -ketoenamine-linked COFs (Scheme 2). First, the initial reaction of Tp with Py is favoured due to the higher basicity compared to aromatic amines. After

Scheme 2 The proposed mechanism of Py-assisted transimination for the synthesis of the  $\beta$ -ketoenamine-linked COF.

an enol-to-keto tautomerization, the formed tertiary amine in compound **II** should be exceptionally stable and in turn, modulate the following transimination between iminium **I** and aromatic amines to produce the compounds **III** and **IV**. Therefore, it is assumed that Py may enhance the controllability of the crystal growth kinetics, resulting in a better crystalline structure of  $\beta$ -ketoenamine-linked COFs.

In summary, we present an organobase-assisted method to synthesize a variety of  $\beta$ -ketoenamine-linked COFs with high-quality crystallinity and porosity. Pyrrolidine instead of acetic acid aqueous solution plays a role as a modulator in the synthesis to allow the improvement of structural ordering and intrinsic porosity. Also, it is proved that a variety of organobases have a similar effect and pyrrolidine is the most efficient. Adaptability of pyrrolidine has been manifested by successfully synthesizing nine kinds of  $\beta$ -ketoenamine-linked COFs. The quality of most COFs outperforms those using HOAc aqueous solution. Thus, the mechanism of an iminium-mediated transimination is proposed to understand the organobase-modulated synthesis of COFs. Our study would provide much impetus for exploration of high-quality  $\beta$ -ketoenamine-linked COFs towards advanced applications such as catalysis and energy storage.

We acknowledge the financial support of the NSFC (21774023, 51973039 and 51633001) and STCSM (18520744800).

## Conflicts of interest

There are no conflicts to declare.

## Notes and references

- 1 A. P. Côté, A. I. Benin, N. W. Ockwig, M. O'Keeffe, A. J. Matzger and O. M. Yaghi, *Science*, 2005, **310**, 1166.
- 2 K. Geng, T. He, R. Liu, K. T. Tan, Z. Li, S. Tao, Y. Gong, Q. Jiang and D. Jiang, *Chem. Rev.*, 2020, **120**(16), 8814.
- 3 P. J. Waller, S. J. Lyle, T. M. Osborn Popp, C. S. Diercks, J. A. Reimer and O. M. Yaghi, *J. Am. Chem. Soc.*, 2016, **138**, 15519.
- 4 H. Liu, J. Chu, Z. Yin, X. Cai, L. Zhuang and H. Deng, *Chemistry*, 2018, **4**, 1696.
- 5 F. Haase, E. Troschke, G. Savasci, T. Banerjee, V. Duppel, S. Dörfler, M. M. J. Grundei, A. M. Burow, C. Ochsenfeld, S. Kaskel and B. V. Lotsch, *Nat. Commun.*, 2018, **9**, 2600.
- 6 X. Li, C. Zhang, S. Cai, X. Lei, V. Altoe, F. Hong, J. J. Urban, J. Ciston, E. M. Chan and Y. Liu, *Nat. Commun.*, 2018, **9**, 2998.
- 7 E. Jin, M. Asada, Q. Xu, S. Dalapati, M. A. Addicoat, M. A. Brady, H. Xu, T. Nakamura, T. Heine, Q. Chen and D. Jiang, *Science*, 2017, **357**, 673.
- 8 (a) X. Zhuang, W. Zhao, F. Zhang, Y. Cao, F. Liu, S. Bi and X. Feng, *Polym. Chem.*, 2016, **7**, 4176; (b) S. Bi, C. Yang, W. Zhang, J. Xu, L. Liu, D. Wu, X. Wang, Y. Han, Q. Liang and F. Zhang, *Nat. Commun.*, 2019, **10**, 2467.
- 9 J. Guo, Y. Xu, S. Jin, L. Chen, T. Kaji, Y. Honsho, M. A. Addicoat, J. Kim, A. Saeki, H. Ihee, S. Seki, S. Irle, M. Hiramoto, J. Gao and D. Jiang, *Nat. Commun.*, 2013, **4**, 2736.
- 10 C. R. DeBlase, K. E. Silberstein, T.-T. Truong, H. C. D. Abruna and W. R. Dichtel, *J. Am. Chem. Soc.*, 2013, **135**, 16821.
- 11 (a) S. Kandambeth, A. Mallick, B. Lukose, M. V. Mane, T. Heine and R. Banerjee, *J. Am. Chem. Soc.*, 2012, **134**, 19524; (b) B. P. Biswal, S. Chandra, S. Kandambeth, B. Lukose, T. Heine and R. Banerjee, *J. Am. Chem. Soc.*, 2013, **135**, 5328.
- 12 S. Wang, Q. Wang, P. Shao, Y. Han, X. Gao, L. Ma, S. Yuan, X. Ma, J. Zhou, X. Feng and B. Wang, *J. Am. Chem. Soc.*, 2017, **139**, 4258–4261.
- 13 S. Gu, S. Wu, L. Cao, M. Li, N. Qin, J. Zhu, Z. Wang, Y. Li, Z. Li, J. Chen and Z. Lu, *J. Am. Chem. Soc.*, 2019, **141**(24), 9623.
- 14 J. H. Chong, M. Sauer, B. O. Patrick and M. J. MacLachlan, *Org. Lett.*, 2003, **5**, 3823.
- 15 M. C. Daugherty, E. Vitaku, R. L. Li, A. M. Evans, A. D. Chavez and W. R. Dichtel, *Chem. Commun.*, 2019, **55**, 2680.
- 16 S. Morales, F. G. Guijarro, J. L. G. Ruano and M. B. Cid, *J. Am. Chem. Soc.*, 2014, **136**, 1082.
- 17 N. C. Flanders, M. S. Kirschner, P. Kim, T. J. Fauvell, A. M. Evans, W. Helweh, A. P. Spencer, R. D. Schaller, W. R. Dichtel and L. X. Chen, *J. Am. Chem. Soc.*, 2020, **142**, 14957–14965.
- 18 S. Ghosh, A. Nakada, M. A. Springer, T. Kawaguchi, K. Suzuki, H. Kaji, I. Baburin, A. Kuc, T. Heine, H. Suzuki, R. Abe and S. Seki, *J. Am. Chem. Soc.*, 2020, **142**, 9752.
- 19 (a) T. Ma, E. A. Kapustin, S. X. Yin, L. Liang, Z. Zhou, J. Niu, L.-H. Li, Y. Wang, J. Su, J. Li, X. Wang, W. D. Wang, W. Wang, J. Sun and O. M. Yaghi, *Science*, 2018, **361**, 48; (b) Q. Zhu, X. Wannig, R. Clowes, P. Cui, L. Chen, M. A. Little and A. I. Cooper, *J. Am. Chem. Soc.*, 2020, **142**, 16842.